

# Computer Simulation Studies of Trishomocubane Heptapeptide of the Type Ac-Ala<sub>3</sub>-Tris-Ala<sub>3</sub>-NHMe

Parvesh Singh<sup>a</sup>, Krishna Bisetty<sup>a,\*</sup>, Penny Govender<sup>b</sup> and Gert Kruger<sup>c</sup>

<sup>a</sup>Department of Chemistry, Durban University of Technology, Steve Biko campus, P.O. Box 1334, Durban, 4000 South Africa.

<sup>b</sup>Department of Chemistry, University of Johannesburg, South Africa.

<sup>c</sup>School of Chemistry, University of KwaZulu-Natal, Durban, 4041 South Africa.

Received 1 March 2011, revised 4 April 2011, accepted 25 May 2011.

Submitted by invitation to celebrate 2011 the 'International Year of Chemistry'.

## ABSTRACT

As part of an extension on the cage peptide chemistry, the present work involves an assessment of the conformational profile of trishomocubane heptapeptide of the type Ac-Ala<sub>3</sub>-Tris-Ala<sub>3</sub>-NHMe using molecular dynamics (MD) simulations. All MD protocols were explored within the framework of a molecular mechanics approach using the PARM94 force field parameters modified in-house to mimic the implicit and explicit solvent conditions. The 50 ns MD trajectories revealed a tendency of the trishomocubane polypeptide to adopt bent conformations *in vacuo*, MEOH and TIP3P solvent models, consistent with previous studies undertaken in our laboratory. The aim of this paper is to exemplify the tendency of the highly constrained cage residues to promote reverse-turn characteristics in the polypeptide chains, which could play a pivotal role in the design of new cage peptidomimetics.

## KEYWORDS

Trishomocubane, molecular dynamics, Amber, CLASICO,  $\beta$ -turn,  $\alpha$ -helical.

## 1. Introduction

Trishomocubanes have a unique cage-like structures due to their D<sub>3</sub> stereoisomerism with similar conformational properties to the pentacycloundecanes (PCUs) and with their ability to be used as multiple drug targets.<sup>1</sup> Specifically, the unnatural cage amino compounds are known to exhibit a range of bioactive characteristics that could enhance the activity of the novel bioactive trishomocubane (TRIS) and the pentacyclo-undecane (PCU) cage amino compounds. Moreover, the rigid cage structures in some of the PCU amino compounds are known to induce receptor site specificity in areas such as antibacterial activity, anabolic action and analgesic activity.<sup>2–4</sup> Literature studies on anti-parkinsonian activity revealed that trishomocubanes showed anti-cataleptic activity in the range of 10 to 34 mg/kg for ED50, as well as anticholinergic activity in the range of 10 to 100 mg/kg.<sup>5</sup> In addition to the anti-parkinsonian activity, anti-viral activity was also seen for these cage compounds.<sup>5</sup> Moreover, the inherent steric bulk of the rigid cage structures could potentially be advantageous in slowing down the drug degradation, thus making drug administration to patients less frequent. In order to understand the function of the peptides and proteins in biological processes, knowledge of their molecular structure is an essential prerequisite. Therefore, structural investigations on these novel compounds are crucial.

Our initial gas-phase studies<sup>6–8</sup> on (R)-8-amino-pentacyclo [5.4.0.02,6.03,10.05,9] undecane-8-carboxylic acid mono-peptide (PCU cage mono-peptide), and on trishomocubane, T4-amino-(D3)-trishomocubane-4-carboxylic acid (TRIS-amino acid residue) revealed the presence of four low-energy conformers, C<sub>7ax</sub>, C<sub>7eq</sub>,  $\alpha_R$  and  $\alpha_L$  located on their conformational spaces depicted in Fig. 1.

These studies also revealed that the highly constrained -amino

acid residues exhibited peculiar conformational characteristics with the model peptides glycine (Gly), L-alanine (Ala) and alpha-aminoisobutyric acid (Aib). Moreover, the peptide sequences were found to be effective at stabilizing the *trans* conformer of the amide bonds between residues (i to i + 1) and (i to i + 2) which satisfy the criteria for reverse-turns and with a strong tendency to promote  $\beta$ -turns.<sup>9</sup>

Our continuous interest in the PCU cage peptide chemistry prompted us to explore the conformational profile of the trishomocubane (TRIS) cage peptides under different environmental conditions. In this paper, we report on the conformational studies of TRIS cage polypeptide chain of the type Ac-Ala<sub>3</sub>-Tris-Ala<sub>3</sub>-NHMe carried out *in vacuo* and in explicit solvents, *viz.* methanol (MEOH) and TIP3P water. The selection of the organic solvents for the present investigations has been made to mimic the dynamic behaviour of these polypeptides under physiological conditions. Accordingly, our aim in this paper is to ascertain the impact of the presence of TRIS cage residues in Ala polypeptide chains of the type Ac-Ala<sub>3</sub>-Tris-Ala<sub>3</sub>-NHMe using MD simulations in different environments. Thus, it is expected that the inclusion of the intervening three Ala residues on either side of the TRIS cage residue (1) would display distinct conformational preferences and hence provide additional information about the conformational characteristics of TRIS cage polypeptides in different environments. Overall it is expected that this study would enhance our understanding of the manipulation of the three-dimensional structures of cage polypeptides.

## 2. Computational Methodology

All MD trajectories were carried out within the framework of molecular mechanics, using the in-house modified all-atom

\* To whom correspondence should be addressed. E-mail: bisettyk@dur.ac.za

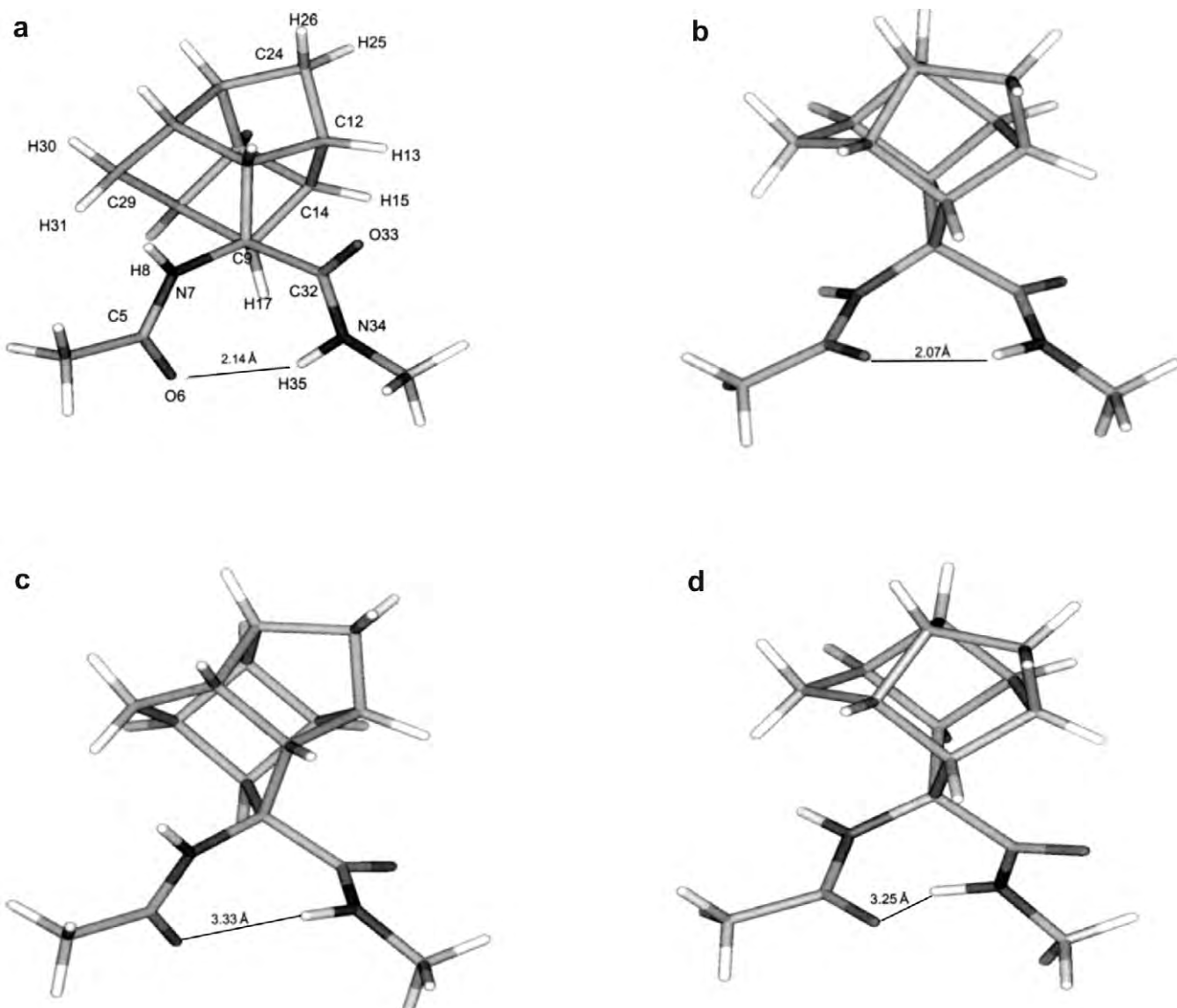


**Figure 1** Low energy conformations (a)  $C_{7\text{eq}}$ , (b)  $C_{7\text{ax}}$ , (c)  $\alpha_R$  and (d)  $\alpha_L$ , of Ac-cage-NHMe.

PARM94 force-field parameters from AMBER 9.0<sup>10</sup>. The Ac-Ala<sub>3</sub>-Tris-Ala<sub>3</sub>-NHMe sequence was built using the ANTE-CHAMBER<sup>11</sup> module of AMBER. The MD simulations were carried out *in vacuo*, water TIP3P model<sup>12</sup>, and then in a box of MeOH molecules. An extended conformation of the Ac-Ala<sub>3</sub>-Tris-Ala<sub>3</sub>-NHMe polypeptide was used as the starting structure, and then minimized using 10 000 steps of steepest descent, followed by a subsequent minimization using the conjugate gradient algorithm until a convergence of the gradient norm was lower than 0.001 kcal mol<sup>-1</sup> Å. The molecule was placed into a rectangular box of TIP3P explicit water molecules with dimensions 36 × 35 × 38 Å<sup>3</sup>. The minimization of these new systems were completed when a convergence criteria (0.001 kcal mol<sup>-1</sup> Å) was reached. Thereafter, periodic boundary conditions<sup>13</sup> were introduced and the structure was allowed to equilibrate for 500 ps at a temperature of 300 K, with the pressure set to 1 bar. SHAKE algorithm was used to constrain all the bonds involving hydrogen atoms with a time step of 2 fs. After the first equilibration phase, the Particle-Mesh Ewald (PME) method<sup>14</sup> was applied with a grid spacing of approximately 1 Å. The equilibration phase involved a single MD trajectory run for 50 ns under these conditions. Similar protocols were used to carry out MD simulations of Ac-Ala<sub>3</sub>-Tris-Ala<sub>3</sub>-NHMe explicitly in MeOH.

### 3. Results and Discussion

The conformational results for the TRIS cage residue occupying positions (i + 2) to (i + 4), respectively in Ac-Ala<sub>3</sub>-Tris-Ala<sub>3</sub>-NHMe, are presented in the Ramachandran plots in Fig. 2a–c. A similarity in the conformational preferences exhibited by each of the Ala segments is observed in all the environments used. However, a closer inspection of the maps revealed that the most striking feature is the restricted nature of the conformational space exhibited by the TRIS cage residue, especially in the presence of TIP3P water model corresponding to the (i + 3) position. This corresponds to the transformation of the initial  $\alpha_L$  conformation into the energetically more favourable  $C_{7\text{eq}}$  conformation (Fig. 2c). A major difference observed in the case of *vacuo* and MeOH (Figs. 2a and 2b, respectively), where the conformational space of TRIS residue was found to be well explored, confirming the existence of the  $C_{7\text{ax}}$ ,  $C_{7\text{eq}}$ ,  $\alpha_R$  and  $\alpha_L$  conformations, in accordance with our previously reported results.<sup>6–8</sup> While the right-handed  $\alpha$ -helix ( $\alpha_R$ ) predominated in MeOH, an equal percentage of each conformer prevailed *in vacuo*. It is assumed that the intermolecular interactions between the peptide residues and solvent molecules especially in the TIP3P solvent restricted the flexibility of the peptide and preferably stabilizes the high energy conformers of the TRIS residue consistent with our previously

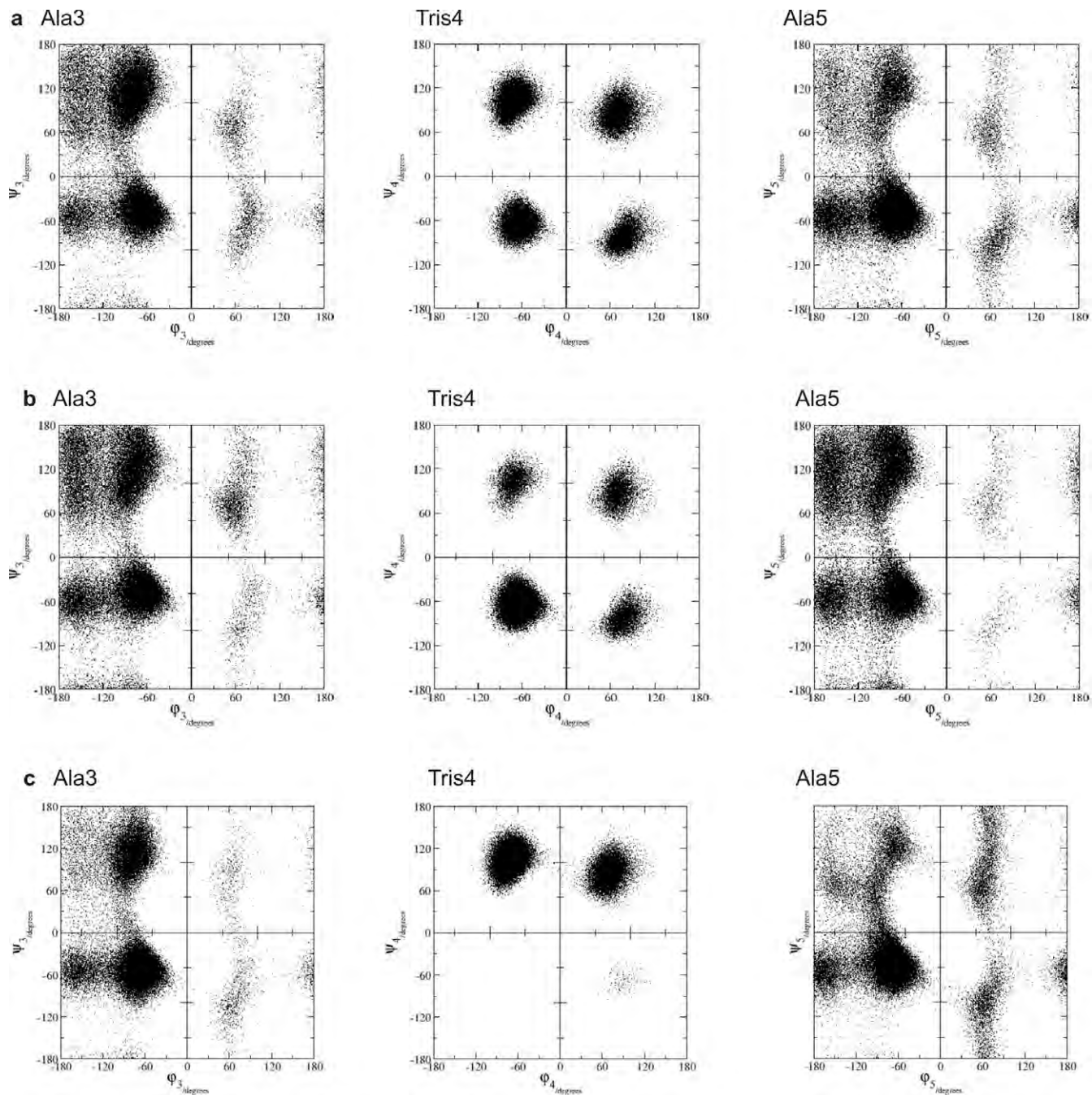


**Figure 2** Ramachandran plots for Ac-Ala<sub>3</sub>-Tris-Ala<sub>3</sub>-NHMe in (a) *vacuo*, (b) MEOH and (c) TIP3P.

reported results on the PCU heptapeptide.<sup>15</sup> On the other hand, the absence of these intermolecular interactions *in vacuo*, make the peptide more flexible resulting in a larger conformational variety of the cage residue.

Figures 3a–3c suggest fluctuations and movement in the backbone torsion angles ( $\phi$  and  $\Psi$ ) of TRIS residue along the MD trajectory *in vacuo*, MEOH and TIP3P, respectively.

A closer inspection of Figs. 3a–3b revealed that the fluctuation of phi (between 80 to –80) and psi angles (100 for 30000 ps and –80 for next 20000 ps) was almost similar *in vacuo* and MEOH solvent clearly suggesting the presence of all four low energy conformations of the TRIS residue in these environments. On the other hand, backbone torsion angles ( $\phi = 80, -80, \Psi = 100$ ) remained relatively fixed in case of TIP3P solvent (Fig. 3c) accounting for lesser conformational variety of TRIS residue in this solvent. The restricted conformations depicted in Fig. 3c is probably due to

the strong intermolecular interactions between the highly polar water molecules and the cage residue, resulting in a higher torsional energy barrier of the central TRIS residue.

In order to further characterize the structural features of Ac-Ala<sub>3</sub>-Tris-Ala<sub>3</sub>-NHMe in different environments, a qualitative analysis of the secondary motifs was performed. For this purpose we used the CLASICO program<sup>16,17</sup> which enables the identification of the secondary motifs from each snapshot. The program translates each snapshot into a string of letters and subsequently computes for each residue its backbone torsion angles, and assigns a letter to it following the Zimmerman partition of the Ramachandran map.<sup>17</sup> Following a set of rules, each string is analyzed using a three-letter window to assign the corresponding secondary motif. Histograms of the secondary motifs per residue for each of the environments used in the present work are depicted in Fig. 4a–c.

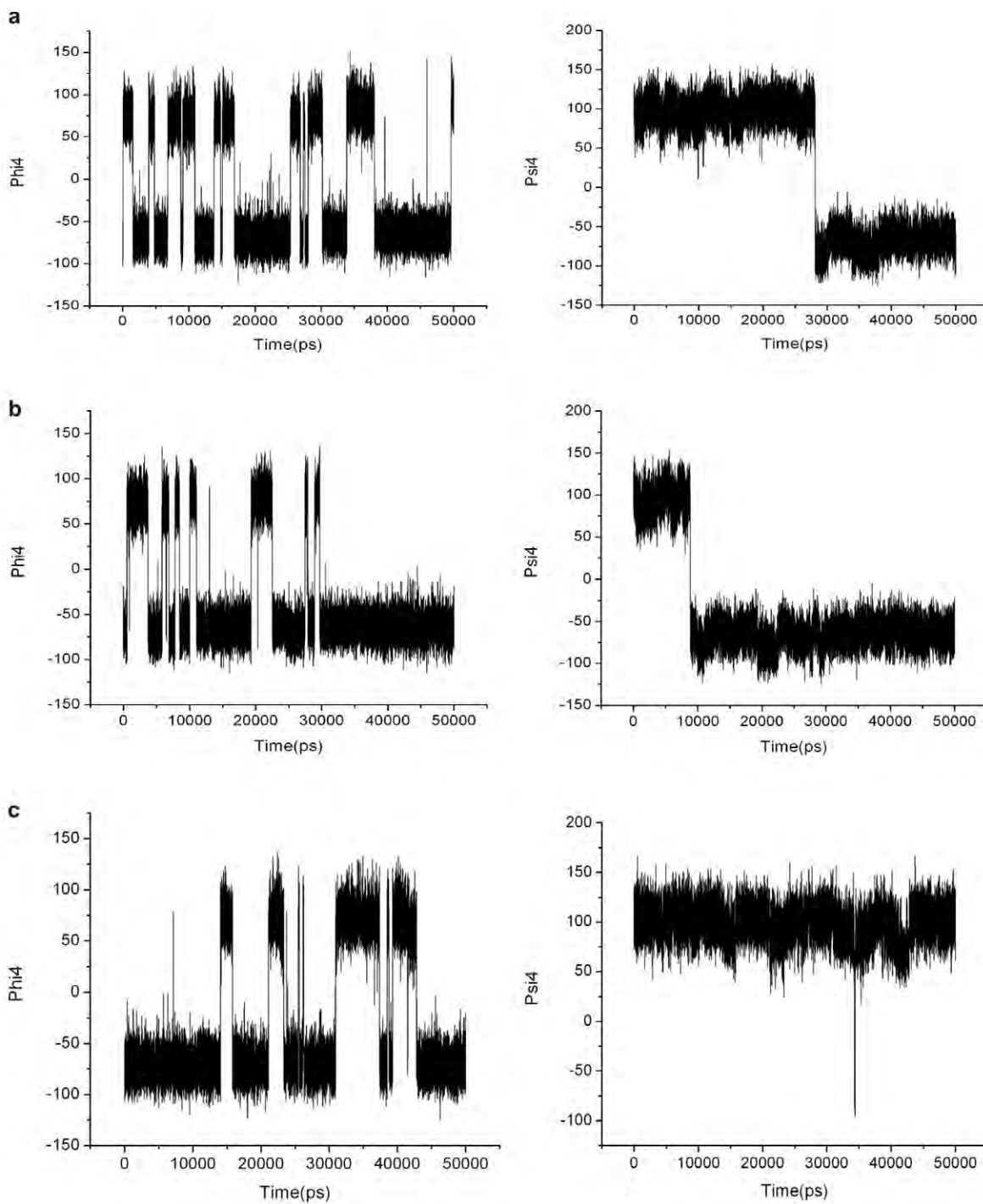


**Figure 3** Backbone torsion angles attained by the TRIS residue in (a) *vacuo* (b) MEOH and (c) TIP3P.

Specifically, the conformational motifs obtained *in vacuo* (Fig. 4a) and methanol (Fig. 4b) show the predominance of  $\beta$ -turn type III ( $3_{10}\text{-}\alpha$  helix) between residues 2 and 6 with a lower propensity observed in the case of the TIP3P water model (Fig. 4c). To some extent,  $\beta$ -turn type I was also observed between residues 2 and 6, both *in vacuo* and in MEOH. Surprisingly, the extent of  $\beta$ -turn exhibited by TRIS cage residue, in TIP3P solvent, was almost negligible (~4 %) in contrast to other environments used for the MD simulations. However, all other Ala residues exhibited both  $\beta$ -turns type III ( $3_{10}\text{-}\alpha$  helix) and I in almost 50 % of the conformations sampled. Overall, these results revealed that the trishomocubane polypeptide predominantly adopts a  $\beta$ -turn type III conformation, irrespective of the environment used for the simulations, but to a lesser extent in TIP3P.

similar to our previous studies carried out on the PCU cage polypeptides.<sup>15</sup> In general, the  $\beta$ -turn profile exhibited by the whole peptide is almost similar in terms of the types (I and III) and their percentages (40–60 %) as depicted in Fig. 4a–c.

Since, hydrogen bonds play a significant role in the folding process of peptides and proteins, the secondary structural features obtained in the current simulations were further rationalized by the hydrogen bond analysis. For this purpose, the coordinates obtained from different trajectories were subjected to the H bond analysis using ptraj module of the AMBER and the CLASICO program.<sup>15</sup> The geometrical criterion used for the donor (A)-acceptor (B) distance is 3.0 Å and the angle HAB ( $\angle$ HAB) is 120 °. In this case, A is donor (i.e. N-H) and B is acceptor (i.e. O of carbonyl group). In order to obtain significant

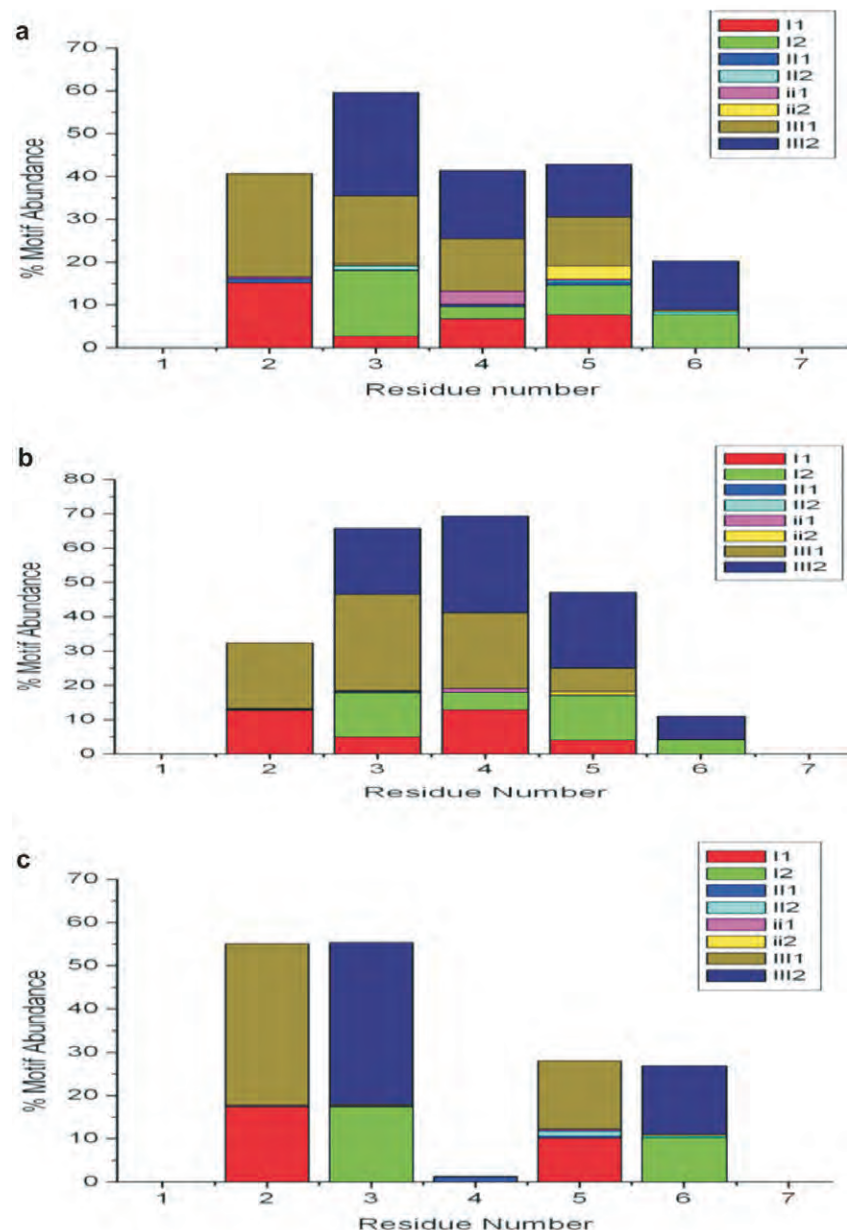


**Figure 4** Type of  $\beta$ -turns attained by the Ac-Ala<sub>3</sub>-Tris-Ala<sub>3</sub>-NHMe peptide in (a) *vacuo* (b) MEOH and (c) TIP3P.<sup>15</sup>

results, only the hydrogen bond with a percentage of existence  $\geq 1.0\%$  was considered. Table 1 summarizes the type of interactions, and percentages of the conformations displaying different secondary structures, for the different environments investigated.

The prevalence of hydrogen bonding patterns along the sampling process, depicted in Fig. 5a–c represents the time evolution of hydrogen bond (HB) formation and breaking during the progress of the MD in each environment. It should be noted that the first specified percentage value of each environment in Table 1 corresponds to the first H-bond distance displayed in Fig. 5a–c. The partial appearance of the initial three hydrogen bonds (labels 1–3, Fig. 5a–c) suggests the presence of  $\alpha$ -helical regions (*i* to *i* + 4 interaction) between residues 1–5, 2–6, and 3–7, respectively in the environments used.

The extent of the helicity was higher *in vacuo* (Table 1) compared to the solvent systems investigated. The hydrogen bonds (labelled 4–7, Fig. 5a–c) account for the different  $\beta$ -turns in the conformations sampled in the different environments used. *In vacuo*,  $\beta$ -turns between residues Ala<sup>1</sup>-Tris<sup>4</sup>, and Tris<sup>4</sup>-Ala<sup>7</sup>

(labelled 4 and 7 in Fig. 5a) were acquired by most of the structures throughout the progress of the trajectory. On the other hand, a  $\beta$ -turn between residues Ala<sup>3</sup>-Ala<sup>6</sup> (labelled 6, Fig. 5b) was predominant in MEOH solvent after 9 ns. In the case of TIP3P (Fig. 5c), two hydrogen bonds (labelled 4 and 5, Table 1) responsible for  $\beta$ -turns between residues Ala<sup>2</sup>-Ala<sup>5</sup>, and Ala<sup>3</sup>-Ala<sup>6</sup>, were attained by most of the structures sampled.

**Table 1** Secondary structural features observed due to backbone-backbone hydrogen bond interactions and their percentages in different environments for Ac-Ala<sub>3</sub>-Tris-Ala<sub>3</sub>-NHMe peptide.<sup>10,16</sup>

Donor–acceptor	2° structure	<i>vacuo</i>	TIP3P	MEOH
(Ala <sup>1</sup> )O...N(Ala) <sup>5</sup>	$\alpha$ -helical	45.9	22.2	24.5
(Ala <sup>2</sup> )O...N(Ala <sup>6</sup> )	$\alpha$ -helical	41.2	25.1	26.5
(Ala <sup>3</sup> )O...N(Ala <sup>7</sup> )	$\alpha$ -helical	47.5	52.3	45.2
(Ala <sup>1</sup> )O...N(Tris <sup>4</sup> )	$\beta$ -turn	38.5	32.7	40.5
(Ala <sup>2</sup> )O...N(Ala <sup>5</sup> )	$\beta$ -turn	47.0	44.6	47.8
(Ala <sup>3</sup> )O...N(Ala <sup>6</sup> )	$\beta$ -turn	34.7	49.9	47.1
(Tris <sup>4</sup> )O...N(Ala <sup>7</sup> )	$\beta$ -turn	37.3	48.8	44.8

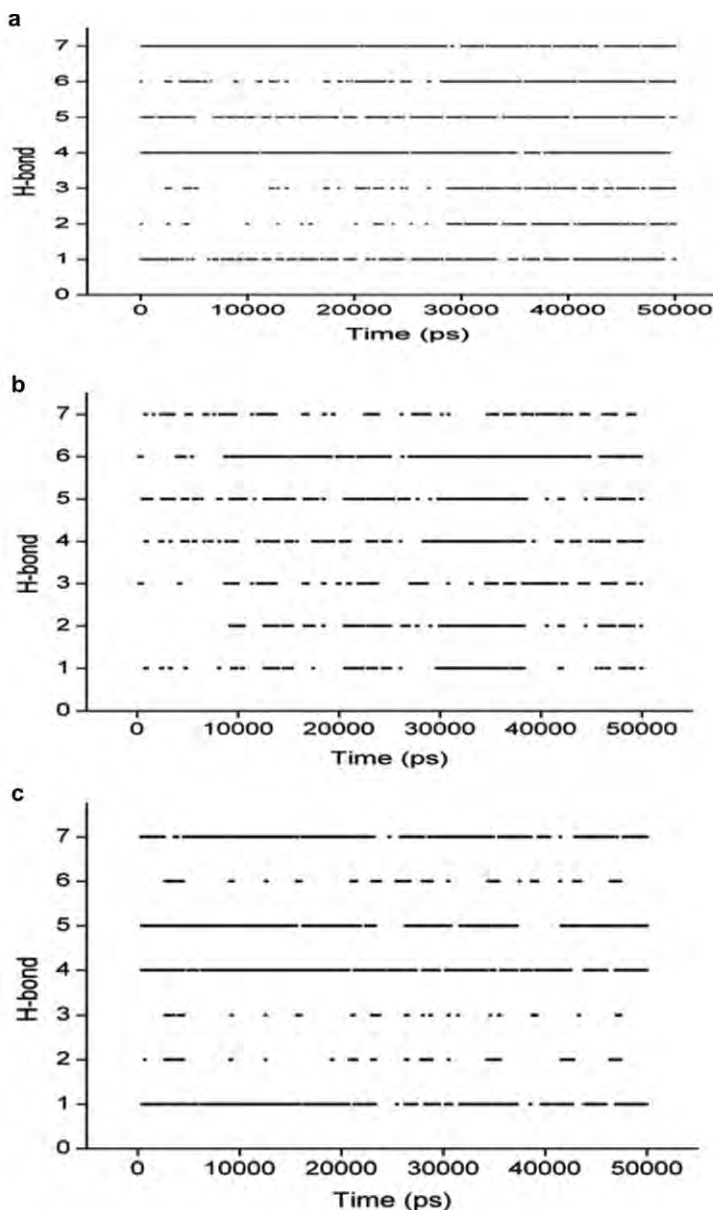


**Figure 5** Progress of hydrogen bonds monitored along the 50 ns trajectory for Ac-Ala<sub>3</sub>-Tris-Ala<sub>3</sub>-NHMe attained in (a) *vacuo* (b) MEOH and (c) TIP3P.<sup>10,16</sup>

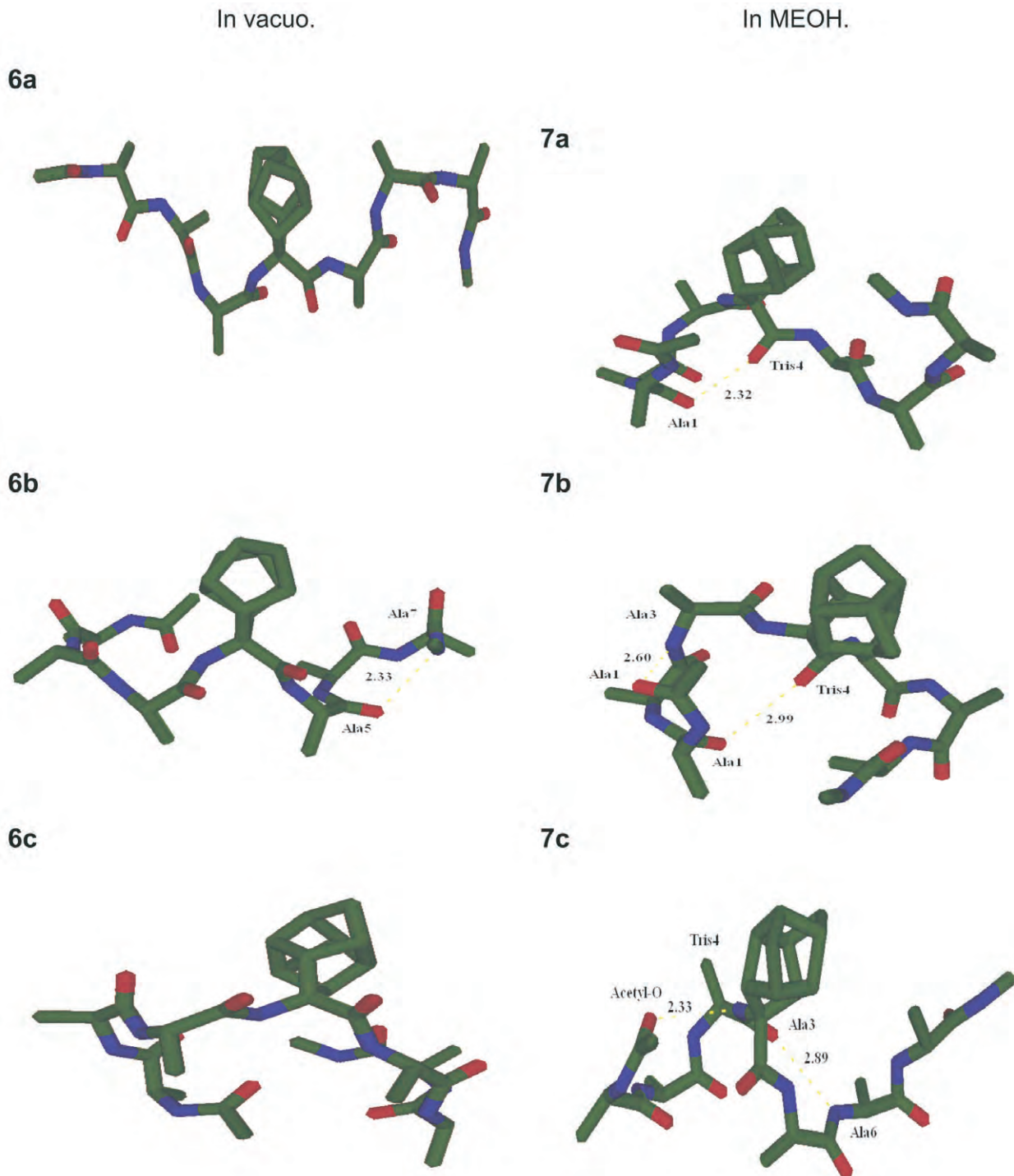
In order to better understand the most populated conformations of the peptide in each MD trajectory, it was considered worthwhile to group all conformations into clusters according to their similarity. For this purpose, 1000 structures of the each MD trajectory were chosen as representative structures considering every snapshot after 50 ps. Ward's hierarchical clustering algorithm<sup>18</sup> was employed to generate clusters using the rmsd of the backbone atoms between two configurations as a distance. The representative structures of three major clusters (containing conformations with most shared secondary motifs) in each MD trajectory are pictorially depicted in Figs. 6–8, while their structural details (percentage of structures, dihedral angles, etc.) are

summarized in Tables 2–4. For Tables 3 and 4 see supplementary data.

A closer inspection of Table 2 revealed that more than 98 % conformations of each trajectory were distributed amongst the three major clusters (I, II and III). However, cluster II was found to be most abundant *in vacuo* (Table 2), while cluster I predominated in the explicit MEOH and TIP3P solvents (Tables 3, 4, see supplementary data). Furthermore, the comparison of the representative structures (RS) of each cluster in different environments suggested that peptide adopts preferably bent conformations in the explicit solvents (Fig. 7a–c and Fig. 8a–c) than in the *vacuo* (Fig. 6a–c) supported by extensive

**Table 2** Structural details of clusters I–III in case of *vacuo*.<sup>18</sup>

Cluster no.	Percentage of structures	Phi angle (for TRIS residue) in RS	Psi angle (for TRIS residue) in RS	Tris conformation in RS
I	30.2	60.5	-75.2	C <sub>7ax</sub>
II	40.1	45.5	60.8	$\alpha_L$
III	27.7	-65.2	74.9	C <sub>7eq</sub>



**Figures 6–7** Representative structures (RS) of three clusters *in vacuo* and in MEOH. Hydrogens are removed for the clarity. Yellow dotted lines show the hydrogen bonds.

intramolecular hydrogen bonding. Additionally, the participation of TRIS residue in hydrogen bonding was more intense in the explicit solvents than in the case of *vacuo*. The monitoring of  $\phi$  (Phi) and  $\Psi$  (Psi) backbone torsion angles of RS *in vacuo* further suggested the presence of three conformations ( $C_{7\text{ax}}$ ,  $\alpha_L$  and  $C_{7\text{eq}}$ ) of TRIS residue for clusters I–III, respectively (Fig. 6a–c). Although, similar conformers of TRIS were observed for clusters I–III in case of MEOH, only two conformers ( $C_{7\text{eq}}$  for cluster I and  $\alpha_L$  for Clusters II and III) were found in the TIP3P (see experimental data) clearly suggesting the lower conformational flexibility of peptide in the water solvent. Overall, these results revealed that the cage peptide has a stronger tendency to adopt  $\beta$ -turns

compared with the helical structures, which are in accordance with those obtained from the secondary structure analysis, described in this paper.

#### 4. Conclusions

The present results revealed that the peptide Ac-Ala<sub>3</sub>-Tris-Ala<sub>3</sub>-NHMe exhibits  $\beta$ -turns as a preferred conformation, irrespective of the environments used. MD simulations performed *in vacuo* were successful in the sampling of the four low energy conformations of the TRIS peptide, as previously described on the basis of quantum mechanics calculations. On other hand, the exploration of the configurational space of the TRIS residue was

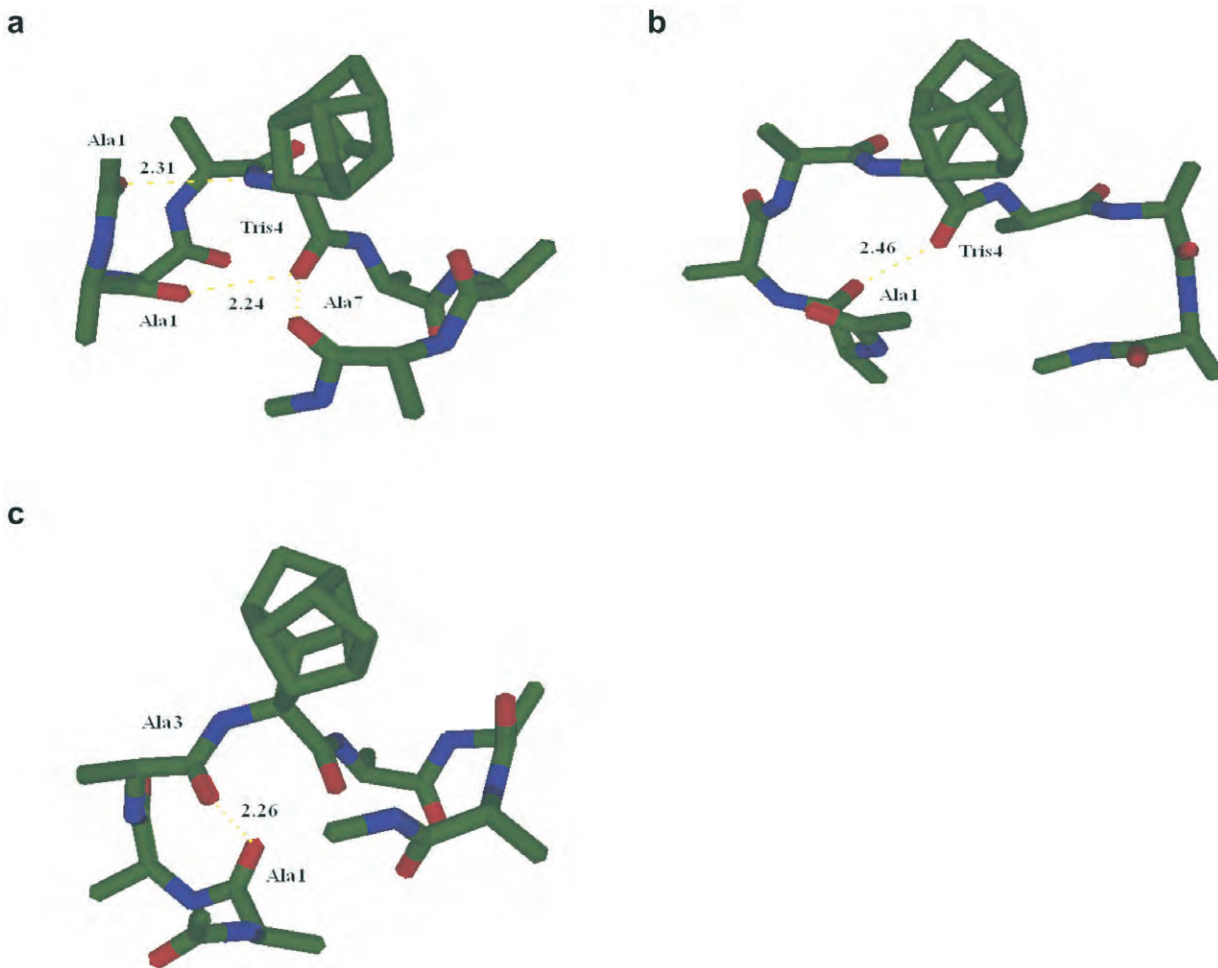


**Figure 8** Representative structures (RS) of three clusters in TIP3P. Hydrogens are removed for the clarity. Yellow dotted lines show the hydrogen bonds.

restricted in the case of explicit solvents especially for the TIP3P solvent model, where only two of the four low energy conformers were explored. Our findings clearly highlight the lower efficiency of the explicit simulations compared to the implicit solvent simulations on the same time scale. Overall, the observed tendency of Ac-Ala<sub>3</sub>-Tris-Ala<sub>3</sub>-NHMe to adopt bent conformations in the presence of a constrained residue is a significant feature that could be invaluable to the general field of peptidomimetics.

#### Acknowledgements

PS gratefully acknowledges financial support from the Durban University of Technology and the National Research Foundation for the position of a Research Associate. KB gratefully acknowledges the experiences and insights gained from the Spanish collaborators (Professor Juan J. Perez and co-workers) through the SA-Spain bilateral agreement.

#### References

- D.W. Oliver and S.F. Malan, Medicinal chemistry of polycyclic cage compounds in drug discovery research, *Med. Chem. Res.*, 2008, **17**, 137–151.
- K. Gerzon and D. Kou, *J. Med. Chem.* 1967, **10**, 189–199.
- R.T. Rapala, R.J. Kraay and K. Gerzon *J. Med. Chem.* 1965, **8**, 580–583.
- A.N. Voldeng, C.A. Bradley, R.D. Kee, E.L. King and F.L. Melder, *J. Pharm. Sci.* 1968, **57**, 1053–1055.
- D.W. Oliver, T.G. Dekker, F.O. Snyckers and T.G. Fourie, *J. Med. Chem.*, 1991, **34**, 851–854.
- K. Bisetty, F.J. Corcho, J. Canto, H.G. Kruger and J.J. Perez, *J. Peptide Sci.* 2006, **12**, 92–105.
- K. Bisetty, J. Gomez-Catalan, C. Aleman, E. Giralt, H.G. Kruger and J.J. Perez, *J. Peptide Sci.*, 2004, **10**, 274–284.
- K. Bisetty, P. Govender and H.G. Kruger, *Biopolymers*, 2006, **81**, 339–349.
- G.D. Rose, L.M. Giersch and J.A. Smith. *Adv. Protein Chem.*, 1985, **37**, 1–109.
- D.A. Case, T.A. Darden, T.E. Cheatham III, C.L. Simmerling, J. Wang, R.E. Duke, R. Luo, K.M. Merz, D.A. Pearlman, M. Crowley, R.C. Walker, W. Zhang, B. Wang, S. Hayik, A. Roitberg, G. Seabra, K.F. Wong, F. Paesani, X. Wu, S. Brozell, V. Tsui, H. Gohlke, L. Yang, C. Tan, J. Mongan, V. Hornak, G. Cui, P. Beroza, D.H. Mathews, C. Schafmeister, W.S. Ross, P.A. Kollman. AMBER 9, University of California, San Francisco, 2000.
- J. Wang, R.M. Wolf, J.W. Caldwell, P.A. Kollman and D.A. Case, *J. Comp. Chem.*, 2004, **25**, 1157–1174.
- D.M. York, T.A. Darden and L.G. Pedersen, *J. Chem. Phys.*, 1993, **99**, 8345–8348.
- T. Darden, D. York, and L. Pedersen, *J. Chem. Phys.*, 1993, **98**, 10089–10092.
- A. Bondi, *J. Phys. Chem.*, 1964, **68**, 441–452.
- P. Singh, P. Sharma, K. Bisetty and J.J. Perez, *Molecular Simulation*, 2010, **36**, 1035–1044.
- (a) LaFargaCPL: CLASTERIT: Project Info. Available from: <http://devel.cpl.upc.edu/clusterit>. (b) F. Corcho, J. Canto and J.J. Perez, *J. Comp. Chem.*, 2004, **25**, 1937–1952.
- S.S. Zimmerman, M.S. Pottle, G. Nemethy and H.A. Scheraga, *Macromolecules*, 1977, **10**, 1–9.
- J.H. Ward Jr, *J. Am. Stat. Assoc.* 1963, **58**, 236–244.